

Improvements in Age-Specific Mortality at the Oldest Ages

Trifon I. Missov¹, Silvio C. Patricio¹, and Francisco Villavicencio^{1,2}

¹Interdisciplinary Centre on Population Dynamics, University of Southern Denmark

²Department of Economic, Financial and Actuarial Mathematics, University of Barcelona

Abstract

Age-specific mortality improvements are non-uniform, neither across ages nor across time. We propose a two-step procedure to estimate the rates of mortality improvement (RMI) in age-specific death rates (ASDR) at ages 85 and above for ten European countries from 1950 to 2019. In the first step, we smooth the raw death counts and estimate ASDR using four different methods: one parametric (gamma-Gompertz-Makeham), two non-parametric (P -splines and PCLM), and a novel Bayesian procedure to handle fluctuations resulting from ages with zero death counts. We compare the goodness of fit of the four smoothing methods and calculate the year-to-year ASDR differences according to the best-fitting one. We fit a piecewise linear function to these differences in the second step. The slope in each linear segment captures the average RMI in the respective year range. For each age, we calculate the goodness of fit in the last linear segment to assess how informative the estimated RMI of current mortality change is. The estimated rates of mortality improvement or deterioration (RMI) can be used to make short-term social, health, and social planning, as well as more precise mortality forecasts.

1 Rates of Mortality Improvement (RMI)

Improvements in human survival at older ages result from the extension of lifespans and the postponement of mortality [Zuo et al., 2018], which is part of a larger life-expectancy revolution [Oeppen and Vaupel, 2002]. Deaths are postponed while mortality risks shift

toward higher ages, inevitably leading to age-specific mortality improvements at advanced ages [Christensen et al., 2009, Kannisto et al., 1994, Rau et al., 2008, Vaupel et al., 2021]. In most longevous populations today, it also results in an increasing share of nonagenarians and centenarians, whose mortality dynamics influence to a great extent, the changes in the overall death pattern.

The prospects of longevity, lifesaving, and life expectancy depend on the improvements in age-specific death rates (ASDR), especially at ages above 85, where most deaths in future populations will occur [Vaupel et al., 2021, Meslé and Vallin, 2000, Wilmoth, 2000]. Life-table censoring [Missov et al., 2016], scarcity of deaths, and unsatisfactory data quality make estimating mortality progress at these ages complex [Kannisto et al., 1994, Rau et al., 2008]. In addition there has yet to be a consensus in the literature on the mortality dynamics among the oldest-old. While some studies find evidence for mortality deceleration [Horiuchi and Wilmoth, 1998] even after age 100 [Medford et al., 2019], others point to stagnation in postponing deaths to the oldest ages [Modig et al., 2017]. Using Italian data, for instance, Barbi et al. Barbi et al. [2018] postulate that the risk of dying closely approaches a plateau after age 105. The statistical model used to arrive at this result, though, has been subjected to criticism [Newman, 2018a]. Moreover, it has been argued that data errors are the primary cause of the observed late-life mortality deceleration and plateaus [Newman, 2018b] and that the most recent and reliable data analysis suggests an exponential increase in the risk of death even at very old ages [Gavrilov and Gavrilova, 2019]. Nevertheless, Alvarez et al. Alvarez et al. [2021] estimate sex- and age-specific death rates above 105 years using the most recent data from the International Database on Longevity, IDL International Database on Longevity [2021], with a non-parametric approach: none of the studied populations shows a rapid increase in the hazard of death, and the bigger the sample size for a given country (especially France), the more compelling the evidence of a leveling-off.

The Human Mortality Database, HMD [HMD, 2023], provides detailed, high-quality harmonized mortality data for a wide range of country-years. However, death rates reported in the HMD result from complex processing of raw data, which is especially significant at older ages where several assumptions are needed [Wilmoth et al., 2021]. To better understand the mortality dynamics at older ages, we apply a two-step procedure to estimate the rates of mortality improvement (RMI) at each age from 85 to 109 in ten European countries. First, we address the problem of data quality in death counts and exposures by applying four approaches to estimate ASDR from raw data. Then, we iden-

tify distinct year-ranges of linear increase in ASDR and estimate the slope of each linear segment, which indicates the (average) RMI in the corresponding year-range. The last linear segment reflects the current RMI (CRMI) and the length of the period over which CRMI persists. Depending on the latter, CRMI-estimates can play an essential role in public health strategies and social planning.

2 Data

This study focuses on Czechia, Denmark, France, Germany, Italy, the Netherlands, Poland, Spain, Sweden, and Great Britain to reflect different types of mortality dynamics, different population sizes, and different sources of data collection (register-based vs. census-based). We use raw death counts and exposures from the Human Mortality Database [HMD, 2023] for years from 1950 to 2019 (for Germany: only 1991 to 2019). We do not include data from 2020 or 2021, where available, as the age-specific death rates in these years are affected by the COVID-19 pandemic. Mortality deterioration due to COVID-19 and its subsequent recovery has been thoroughly studied [see, for example, Aburto et al., 2022, Schöley et al., 2022], but it is beyond the scope of this paper. We are interested in the overall trend of RMI, namely whether mortality improvements occur at the oldest ages and how persistent they are. We do not consider data for cohorts because their raw death counts are unavailable, and the resulting death-rate patterns are already smoothed by the HMD [Wilmoth et al., 2021].

3 Methods for Estimating Death Rates from Raw Data

As reported in the Methods Protocol of the Human Mortality Database, most raw data require various adjustments before being used as inputs to calculate death rates and build life tables. The most common adjustments are distributing deaths of unknown age proportionately across the age range and splitting aggregate data into finer age categories [Wilmoth et al., 2021]. Among the oldest-old, data quality issues are even more noticeable, with the problem of having zero death counts at some ages. In addition, the HMD makes several assumptions in estimating death rates at older ages. First, observed sex-specific death rates at ages 80 and above are smoothed by fitting a Kannisto model of old-age mortality [Thatcher et al., 1998], which is a logistic curve with an asymptote at 1. Fitted rates are used for all ages above 95 years, regardless of the observed death counts.

For ages 80–95, within each country-year and sex observed, death rates are used up to the last age Y with at most 100 male or 100 female deaths; observed rates are replaced by the fitted ones for ages above Y [Wilmoth et al., 2021].

These and other adjustments in the HMD justify exploring alternative methods to estimate death rates from raw data. Note, for instance, that the Kannisto model implicitly assumes a mortality deceleration at older ages and the existence of a plateau at 1. In the first step, we smooth the raw death counts and estimate ASDR for ages 85–109 using four different methods: one parametric (gamma-Gompertz-Makeham), two non-parametric (P -splines and PCLM), and a novel Bayesian procedure to handle fluctuations resulting from ages with zero death counts. We compare the goodness of fit of the four smoothing methods and calculate the year-to-year ASDR differences according to the best-fitting one. In the second step, we fit a piecewise linear function to these differences. We carry out all our analyses using the open-source statistical software R [R Core Team, 2021].

3.1 Gamma-Gompertz-Makeham model

The gamma-Gompertz-Makeham (ΓGM) is a parametric mortality model that has been widely used in the literature [see, for instance, Vaupel et al., 1979, Vaupel and Missov, 2014]. It is a more flexible version of the Kannisto model [Thatcher et al., 1998] used by the HMD that allows for any positive asymptote. The mortality hazard of the ΓGM model is given by

$$\mu_x = \frac{\alpha e^{\beta x}}{1 + \frac{\gamma^\alpha}{\beta} (e^{\beta x} - 1)} + c,$$

where $x \geq 0$ denotes age, and $\alpha, \beta > 0$ and $c, \gamma \geq 0$ are parameters. It is based on the Gompertz model with baseline mortality α and rate of aging β , with the additional feature of capturing the extrinsic mortality (by the Makeham term c) and unobserved heterogeneity (frailty), which is assumed to be gamma distributed with unit mean and variance γ [Vaupel et al., 1979].

The fitting procedure assumes that death counts come from a Poisson distribution with a rate parameter $E_x \mu_x$. Let D_x be the number of deaths in a given age interval $[x, x + 1)$ for $x = 85, \dots, 109$, and E_x the corresponding exposures. For each country-year and sex, we maximize the Poisson log-likelihood

$$\ln \mathcal{L}(\alpha, \beta, c, \gamma; x) = \sum_{x=85}^{109} (D_x \ln \mu_x - E_x \mu_x)$$

For further discussion on the Γ GGM model and its applications, readers are referred to Vaupel and Missov [2014], Missov and Németh [2015], and Ribeiro and Missov [2016].

3.2 Two non-parametric models

We implement two existing non-parametric models to estimate age-specific death rates from raw death counts and exposures: 1) P -splines [Eilers and Marx, 1996], and 2) PCLM, the penalized composite link method [Rizzi et al., 2015]. Both methods share a common statistical basis, but the latter has been found particularly suitable for reconstructing the tail of a distribution.

1. P -splines are most frequently used for high-precision smoothing of count data. The method is also based on the assumption that data (in this case, deaths) are Poisson-distributed. We use the R package ‘MortalitySmooth’ [Camarda, 2012] to smooth the raw death counts from HMD and estimate the associated ASDR. Readers are referred to Eilers and Marx [1996] and Camarda [2012] for additional details.
2. The PCLM approach is a versatile method to ungroup binned count data, say, age-at-death distributions grouped in age classes. It is based on the idea of P -splines and assumes that counts are Poisson-distributed. We use the ‘ungroup’ R package [Pascariu et al., 2018] to implement the PCLM. Because of zero deaths at some ages, we first sum up all raw death counts of the oldest age groups. In line with the criterion used by the HMD to estimate death rates [Wilmoth et al., 2021], for each country-year and sex, we start the grouping at the first age Y with less than 100 deaths. We then use age-specific death counts for ages 40 to Y from HMD, and the last age-group, $Y+$ with grouped deaths, as an input to PCLM. The PCLM algorithm returns age-specific death counts until the 109-110 age group. We finally use the observed exposures 85–109 from HMD to calculate corresponding age-specific death rates. Readers are referred to Rizzi et al. [2015] and Pascariu et al. [2018] for additional details.

3.3 Bayesian approach

Let us describe in detail the novel Bayesian approach developed for this paper. Suppose D_x is the number of deaths in a given age interval $[x, x + 1)$ for $x = 85, \dots, 109$. For each x , let D_x be Poisson-distributed with $\mathbb{E}D_x = \mathbb{V}D_x = m_x E_x$, where m_x is the central death rate at age x and $E_x > 0$ denotes exposure in $[x, x + 1)$, i.e.,

$$\mathbb{P}(D_x = d) = \frac{(m_x E_x)^d e^{-m_x E_x}}{d!}.$$

For each x , the likelihood function of D_x is given by

$$\mathcal{L}(m_x | D_x = d) = m_x^d e^{-m_x E_x}.$$

Assuming a non-informative or uniform prior distribution for m_x , we get a posterior distribution given by

$$f(m_x | D_x = d) = \frac{E_x^d}{\Gamma(d + 1)} m_x^{(d+1)-1} e^{-m_x E_x},$$

which is equivalent to a gamma distribution with parameters $\kappa = d + 1$ and $\lambda = E_x$. As a result, to estimate m_x , we can use any of the following:

1. the maximum of the posterior distribution, i.e., $\operatorname{argmax}_{m_x} f(m_x | D_x = d)$
(equivalent to MLE, the maximum-likelihood estimate)
2. the expected value of the posterior distribution, i.e., $\frac{d+1}{E_x}$
3. the median of the posterior distribution, i.e., $\left\{ x : \int_0^x f(m_x | D_x = d) = 0.5 \right\}$

As we assume that D_i and D_j are independent for any $i \neq j$, we do not impose any structure on the age axis. The likelihood function, from which the posteriori distribution for m_x is built, comes from a single observation. Therefore, despite providing a good approximation for the risk of dying when $D_x = 0$, this method might be sensitive to outliers, commonly observed after age 100, given the low corresponding exposures E_x .

4 Methods for Estimating Mortality Improvement by Age

After estimating the death rates at ages 85–109 by the four methods described in Section 3 (step 1), we use further the m_x estimates according to the best-fitting model. The goodness of fit criterion we apply is the root-mean-square error (RMSE). As year-to-year differences in m_x can fluctuate, even if we take second or higher-order differences, for each x , we fit, as a second step, a linear regression to log-mortality for $t = 1950, \dots, 2019$:

$$\ln m_x(t) = a + bt. \quad (1)$$

The slope b accounts for the average rate of mortality improvement (if b is negative) or deterioration (if b is positive). A simple linear model fits well only $\ln m_x$ -patterns with a steady trend. When the latter is not present, a natural extension would be to fit a segmented regression [Muggeo, 2003], i.e., to assume that $\ln m_x$ has a piecewise-linear structure over time. The slope in the latest time segment would then reflect the average rate of current mortality change (CRMI). Applying a conventional segmented regression might result in too fine partitioning of the year-axis and wide uncertainty intervals for the RMI as the response variable, the expectation of the logarithmic death rates, is sensitive to mortality fluctuations and outliers. As mentioned, the latter is common at the oldest ages with small E_x -values. We suggest considering the median (instead of the expectation) of $\ln m_x(t)$ to overcome this problem. The median is still a central tendency measure but also robust to extreme values (outliers). As a result, we fit a linear quantile regression, the median of $\ln m_x(t)$ being the response, with an unknown number of breakpoints. We will call it a *segmented quantile regression*. Even though it has already been applied in Tomal and Ciborowski [2020], all statistical properties and technicalities are described in Patricio et al. [2023]. Figure 1 shows how conventional segmented regression responds to outliers at the study period’s beginning, middle, and end. When estimating CRMI, a single outlier in the very last year, like the one for German females at age 100 (Figure 1, middle panel), creates a new breakpoint in the case of segmented regression. This point defines a new final segment with a steep decline in RMI. On the other hand, the segmented quantile regression remains resistant to this outlier and suggests a much more modest CRMI.

The average rate of mortality improvement in the last log-linear segment, the CRMI, is the most informative regarding mortality forecasts and social and health planning. If researchers and policymakers want to use it, assessing the corresponding goodness of fit is important. For that, we use the metric proposed in Koenker and Machado [1999], the

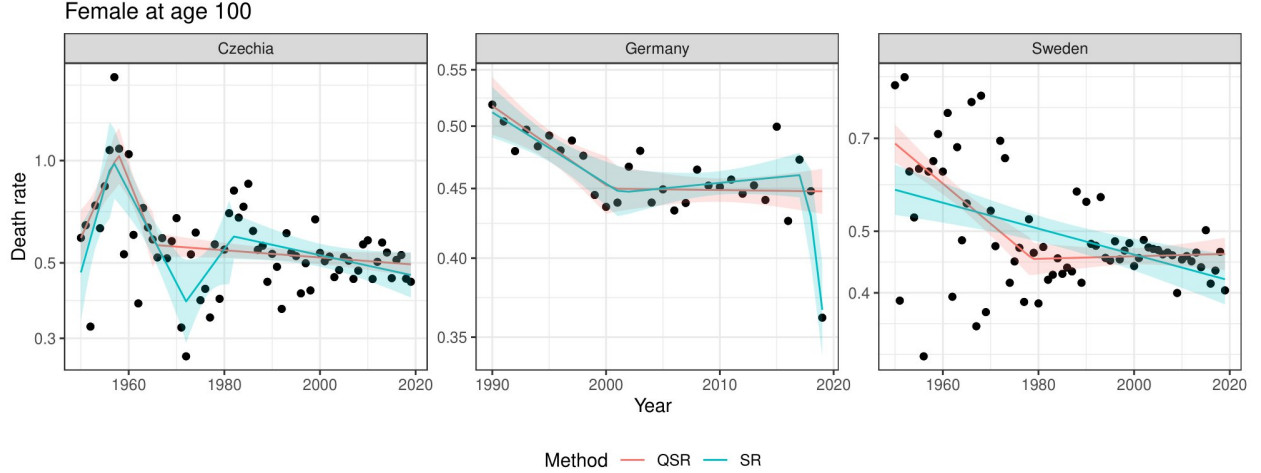


Figure 1: Segmented (in blue) vs segmented quantile regression (in red) fits to $\ln m_{100}(t)$ -series for females in Czechia, Germany, and Sweden. Examples of the sensitivity of conventional quantile regression to outliers are in the beginning (right panel), in the middle (left panel), and at the end (middle panel) of the study period.

pseudo- R^2 , given by

$$R_1(0.5) = 1 - \frac{\sum_{y_i \geq \hat{y}_i} |y_i - \hat{y}_i| + \sum_{y_i < \hat{y}_i} |y_i - \hat{y}_i|}{\sum_{y_i \geq \bar{y}_i} |y_i - \bar{y}_i| + \sum_{y_i < \bar{y}_i} |y_i - \bar{y}_i|},$$

where \hat{y}_i is the fitted median for the observation i , and \bar{y}_i is the fitted value from the intercept-only model. Likelihood ratio tests are carried out using the asymmetric Laplacean density. All technical details can be found in Koenker and Machado [1999].

5 RMI by Sex for 10 European Countries in 1950–2019

For each of the ten European countries and in each year from 1950 to 2019, we estimate the age-specific death rates m_x by each of the four smoothing methods described in Section 3: FGM, P -splines, PCLM and the novel Bayesian procedure. We compare the goodness of fit of the four models by the root-mean-square error (RMSE) and take the smoothed $\ln m_x$ from the best-fitting model (see Table 1). Then, for each series of smoothed $\ln m_x$, we fit a simple linear and segmented quantile regression. We determine the better-fitting regression model by applying a likelihood ratio test (see the resulting piecewise linear fits to the smoothed in step 1 $\ln m_x$ in Figures 3-12 of the Appendix).

Table 2 shows the estimates of CRMI, the average rate of mortality improvement at

Sex	Country	Γ GM	P -spline	PCLM	Bayesian	Best
Female	Czechia	0.71109	0.73121	0.71189	70.58017	Γ GM
Female	Germany	0.15174	0.10589	0.17938	0.08894	Bayesian
Female	Denmark	0.59029	0.60201	0.59611	36.38742	Γ GM
Female	France	0.50288	0.51406	0.49271	275.39504	PCLM
Female	U.K.	0.27511	0.26141	0.28093	1.12509	P -spline
Female	Italy	0.38664	0.35499	0.39471	5.74553	P -spline
Female	Netherlands	0.49128	0.52711	0.50099	1456.71440	Γ GM
Female	Poland	0.51929	0.52108	0.52217	55.98287	Γ GM
Female	Spain	0.15198	0.10612	0.14529	0.06501	Bayesian
Female	Sweden	0.45511	0.52355	0.46491	306.05907	Γ GM
Male	Czechia	0.78001	0.79969	0.78262	578.35638	Γ GM
Male	Germany	0.39312	0.35414	0.40493	5.58635	P -spline
Male	Denmark	0.60277	0.72942	0.63123	85.06176	Γ GM
Male	France	0.52562	0.50671	0.53359	25.46410	P -spline
Male	U.K.	0.39691	0.37715	0.41085	17.78488	P -spline
Male	Italy	0.45973	0.43200	0.47150	11.36622	P -spline
Male	Netherlands	0.58263	0.58902	0.59399	660.47474	Γ GM
Male	Poland	0.45450	0.44954	0.46317	65.65627	P -spline
Male	Spain	0.33390	0.31520	0.37282	0.89869	P -spline
Male	Sweden	0.65804	0.70141	0.67254	85.73861	Γ GM

Table 1: Model-specific root-mean-square errors (RMSE) by country and sex. The best fitting model is listed in the last column.

ages 85, 90, 95, 100, and 105, respectively, by country and sex in the latest time segment (equal to the entire 1950–2019 range if a simple linear regression fits better). Table ?? contains the lengths of the last linear segment in each case. At age 85, the point estimates vary from -0.0228 (Polish females; length of the latest year-segment, L , equal to 24 years) to -0.0108 (Danish females; $L = 49$). At age 90 mortality progress is more modest: from -0.0163 (Polish females; $L = 26$) to -0.0056 (Italian females; $L = 15$). At age 95, gains are even smaller: we have CRMI point estimates from -0.0109 (Polish females; $L = 25$) to -0.0028 (Danish males; $L = 25$). At these ages, the populations in all ten countries, apart from Dutch males at age 90, experience statistically significant mortality improvement

(no confidence interval contains 0). CRMI for females slightly dominates the CRMI for males.

At age 100 (Figure 2, left panel in the second row), 12 out of 20 populations show statistically significant mortality improvement, the CRMI point estimates varying from -0.0071 (French females; $L = 69$) to -0.0012 (Swedish males; $L = 69$). Seven of the remaining populations experience mortality stagnation at age 100, while death rates for Polish males increase in time at a rate of 0.0016 ($L = 51$). This confirms the findings by Modig et al. [2017] and Medford et al. [2019] that mortality progress at 100, if any, is very slow. At age 105, though, Czech females experience the highest mortality improvement with a CRMI of -0.0091 , $L = 36$ (Figure 2, right panel in the second row). Three other populations are making progress in reducing death rates at 105, at a pace equal to -0.0077 (French females; $L = 69$), -0.0025 (Italian females; $L = 69$), and -0.0017 (Dutch males; $L = 69$). Two populations suffer from statistically significant mortality deterioration in the latest time segment: Spanish females with an average CRMI of 0.0030 and Dutch females with an average CMRI of 0.0054 . The CMRI for all other populations indicates mortality stagnation at age 105, the point estimates showing, in most cases, slight increases in the death rates.

The estimated CRMI can be meaningful in mortality forecasting, health, and social planning if a linear model fits the data in the last segment well. Table 3 presents the corresponding pseudo- R^2 values by country, sex, and age. While the linear model captures with high precision CRMI dynamics at ages 85 and 90 (most pseudo- R^2 values being higher than 0.9, see Table 2), it becomes less accurate at age 95. In contrast, at ages 100 and 105, it fits well only for a handful of populations. This implies that it is safe to use the estimated CRMI only at ages 85, 90, and perhaps 95. In contrast, at ages 100 and 105, researchers and policymakers may consider CRMI-estimates only for those populations where the pseudo- R^2 values are high enough (for the purpose CRMI are used).

6 Discussion

The rise of human longevity is one of the major achievements of modern societies. As people live longer and life expectancy increases [Oeppen and Vaupel, 2002], more deaths are concentrated at higher ages [Zuo et al., 2018], and a more profound knowledge of the mortality dynamics among the oldest-old is necessary. Historically, death rates have improved steadily in many countries thanks to advancements in medicine, sanitation, and

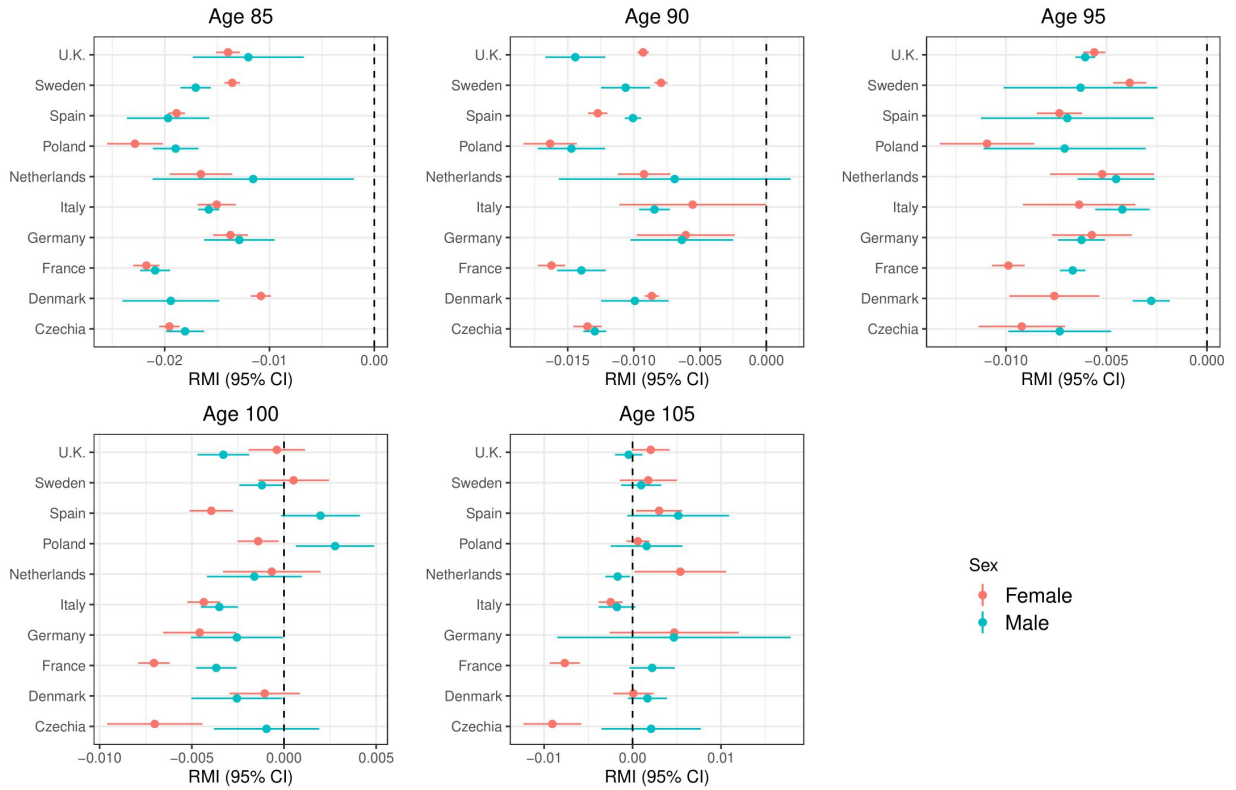


Figure 2: The average rate of mortality improvement at ages 85, 90, 95 (top row), 100 and 105 (bottom row) with 95% uncertainty intervals (males in blue, females in red), calculated as the slope of a segmented quantile regression for the median of $\ln m_x$, estimated by the best-fitting procedure according to Table 1.

lifestyle. However, the degree to which mortality continues to improve after a certain age has been debated among demographers and epidemiologists.

Estimating the rates of mortality improvement (RMI) at the oldest ages has become increasingly important as most deaths, mainly in high-income countries, already take place above age 85. Japanese females, for instance, reached a life expectancy at birth of 87.74 years in 2020 [HMD, 2023], so RMI above that age can play a crucial role in social, medical, actuarial, and pension planning. Also, in population forecasting, provided that in societies with very low neonatal, infant, and child mortality levels, future life expectancy gains will mainly depend on improvements in mortality at older ages [Vaupel et al., 2021].

The scarcity and quality of historical data at these ages call for using models to estimate age-specific death rates (ASDR). This paper explores four approaches: one parametric (gamma-Gompertz-Makeham), two non-parametric (P -splines and PCLM), and a novel Bayesian model. We first choose the best-fitting of the four models for each population to smooth the raw death counts. Then, based on the latter and the exposures, we calculate smoothed ASDR and fit a segmented quantile regression. We get the point estimate of the CRMI, the slope in the last linear segment, and a corresponding uncertainty interval. CRMI reflects current mortality improvement (or deterioration) and is essential in short-term planning and forecasting. Using the estimated CRMI, for instance, in a forecast is sensible when the associated linear trend is persistent. To check the latter, we calculate a pseudo- R^2 in the last segment.

The smoothing step identifies the Γ GMM and the P -splines as the best-fitting models to the raw death counts. While the novel Bayesian procedure sometimes provides the lowest RMSE, in most cases, its RMSE-values are extremely large. In ages with zero reported deaths ($D_x = 0$) in which the respective exposures (E_x) are very small, the expected value of the posterior distribution becomes very large. In general, as we impute a uniform random value u for E_x , the Bayesian method estimates $1/u$. As u is small and $D_x = 0$, the Bayesian estimates at this age x are very high, which affects the associated RMSE-value.

Our results and estimated CRMI suggest that up to age 100, age-specific death rates decrease in time in all ten countries. After 100, about half of the countries still experience improvements in mortality while it stagnates or slightly deteriorates in the others. Table 2 shows that it is sensible to assume a constant yearly rate of mortality change at ages 85, 90, and 95 in the most recent time segment. The associated pseudo- R^2 values are above 0.8 almost across all populations. After age 100, there is a stagnation in reducing death rates, with only a few exceptions. At age 105, some populations even experience mortality

deterioration. Note that at ages 100 and 105, a linear approximation does not have solid statistical justification. It is to be expected due to the small number of data points the estimation of ASDR at these ages is based on, which is consistent with previous research that quantified significant uncertainty in ASDR above ages 105 and 110 [Alvarez et al., 2021, Villavicencio and Aburto, 2021]. As a result, the CRMI-estimates at ages 100 and 105 are non-informative for forecasting and social planning.

Several factors may contribute to the continued improvement in mortality rates among individuals aged 85 and above. First, advancements in medical technology and treatments have allowed for better management of chronic health conditions, such as heart disease and diabetes, which are common among older adults. In addition, lifestyle factors, such as improved nutrition and increased physical activity, may contribute to better health outcomes in later life. Mortality improvements, however, are not uniform across all population subgroups. Improvements among the oldest-old may be impacted by factors such as access to healthcare, social support, and lifestyle. A related question is whether, as life expectancy increases, the extra years of life are being lived in good health. Studies have shown mixed results depending on the age, population, and measure used [Christensen et al., 2009, Beltrán-Sánchez et al., 2015], also conditioned by the inherent uncertainty in health estimates compared to mortality data [Villavicencio et al., 2021].

Acknowledgments

The research leading to this publication is part of a project that has received funding from the European Research Council (ERC) under the European Union's Horizon 2020 research and innovation program (Grant agreement No. 884328 – Unequal Lifespans). It is also part of a project that has received funding from the ROCKWOOL Foundation through the research project "Challenges to Implementation of Indexation of the Pension Age in Denmark." SCP gratefully acknowledges the support from AXA Research Fund through funding the "AXA Chair in Longevity Research." FV acknowledges funding from the Spanish State Research Agency under the Ramón y Cajal program (grant RYC2021-033979-I).

Conflict of Interests

None.

References

- W. Zuo, S. Jiang, Z. Guo, M.W. Feldman, and S. Tuljapurkar. Advancing front of old-age human survival. *Proceedings of the National Academy of Sciences of USA*, 115(44):11209–11214, 2018. doi: 10.1073/pnas.1812337115.
- J. Oeppen and J.W. Vaupel. Broken limits to life expectancy. *Science*, 296(5570):1029–1031, 2002. doi: 10.1126/science.1069675.
- K. Christensen, G. Doblhammer, R. Rau, and J.W. Vaupel. Ageing populations: the challenges ahead. *The Lancet*, 374(9696):1196–1208, 2009. doi: 10.1016/S0140-6736(09)61460-4.
- V. Kannisto, J. Lauritsen, A.R. Thatcher, and J.W. Vaupel. Reductions in mortality at advanced ages: several decades of evidence from 27 countries. *Population and Development Review*, 20:793–810, 1994. doi: 10.2307/2137662.
- R. Rau, E. Soroko, D. Jasilionis, and J.W. Vaupel. Continued reductions in mortality at advanced ages. *Population and Development Review*, 34(4):747–768, 2008. doi: 10.1111/j.1728-4457.2008.00249.x.
- J.W. Vaupel, F. Villavicencio, and M.-P. Bergeron-Boucher. Demographic perspectives on the rise of longevity. *Proceedings of the National Academy of Sciences of USA*, 118(9):e2019536118, 2021. doi: 10.1073/pnas.2019536118.
- F. Meslé and J. Vallin. Transition sanitaire: tendances et perspectives. *Médecine/sciences*, 16:1161–71, 2000.
- J.R. Wilmoth. Demography of longevity: past, present, and future trends. *Experimental Gerontology*, 35(9–10):1111–1129, 2000. doi: 10.1016/S0531-5565(00)00194-7.
- T.I. Missov, L. Németh, and M.J. Daňko. How much can we trust life tables? Sensitivity of mortality measures to right-censoring treatment. *Palgrave Communications*, 2:15049, 2016. doi: 10.1057/palcomms.2015.49.
- S. Horiuchi and J.R. Wilmoth. Deceleration in the age pattern of mortality at older ages. *Demography*, 35(4):391–412, 1998. doi: 10.2307/3004009.

- A. Medford, K. Christensen, A. Skytthe, and J.W. Vaupel. A cohort comparison of lifespan after age 100 in Denmark and Sweden: Are only the oldest getting older? *Demography*, 56:665–677, 2019. doi: 10.1007/s13524-018-0755-7.
- K. Modig, T. Andersson, J.W. Vaupel, R. Rau, and A. Ahlbom. How long do centenarians survive? Life expectancy and maximum lifespan. *Journal of Internal Medicine*, 282(2): 156–163, 2017. doi: 10.1111/joim.12627.
- E. Barbi, F. Lagona, M. Marsili, J.W. Vaupel, and K.W. Wachter. The plateau of human mortality: Demography of longevity pioneers. *Science*, 360(6396):1459–1461, 2018. doi: 10.1126/science.aat3119.
- S.J. Newman. Plane inclinations: A critique of hypothesis and model choice in barbi et al. *PLoS Biology*, 16(12):e3000048, 2018a. doi: 10.1371/journal.pbio.3000048.
- S.J. Newman. Errors as a primary cause of late-life mortality deceleration and plateaus. *PLoS Biology*, 16(12):e2006776, 2018b. doi: 10.1371/journal.pbio.2006776.
- L.A. Gavrilov and N.S. Gavrilova. New trend in old-age mortality: Gompertzialization of mortality trajectory. *Gerontology*, 65(5):451–457, 2019. doi: 10.1159/000500141.
- J.-A. Alvarez, F. Villavicencio, C. Strozza, and C.G. Camarda. Regularities in human mortality after age 105. *PLoS ONE*, 16(7):e0253940, 2021. doi: 10.1371/journal.pone.0253940.
- International Database on Longevity. French Institute for Demographic Studies (INED) (host), 2021. Available at <https://www.supercentenarians.org/>.
- HMD. Human Mortality Database, 2023. Max Planck Institute for Demographic Research (Germany), University of California, Berkeley (USA), and French Institute for Demographic Studies (France). Available at <http://www.mortality.org> (data downloaded on February 14, 2023).
- J.R. Wilmoth, K. Andreev, D. Jdanov, D.A. Gleij, T. Riffe, et al. Methods protocol for the Human Mortality Database, Version 6. Technical report, University of California, Berkeley, and Max Planck Institute for Demographic Research, Rostock, 2021. Available at <https://www.mortality.org/File/GetDocument/Public/Docs/MethodsProtocolV6.pdf> (retrieved on March 10, 2023).

- J.M. Aburto, J. Schöley, I. Kashnitsky, L. Zhang, C. Rahal, T.I. Missov, M.C. Mills, J.B. Dowd, and R. Kashyap. Quantifying impacts of the COVID-19 pandemic through life-expectancy losses: a population-level study of 29 countries. *International Journal of Epidemiology*, 51(1):63–74, 2022. doi: 10.1093/ije/dyab207.
- J. Schöley, J.M. Aburto, I. Kashnitsky, M.S. Kniffka, L. Zhang, H. Jaadla, J.B. Dowd, and R. Kashyap. Life expectancy changes since COVID-19. *Nature Human Behaviour*, 6(12): 1649–1659, 2022. doi: 10.1038/s41562-022-01450-3.
- A.R. Thatcher, V. Kannisto, and J.W. Vaupel. *The force of mortality at ages 80 to 120*. Odense University Press, Odense, Denmark, 1998.
- R Core Team. *R: A Language and Environment for Statistical Computing*. R Foundation for Statistical Computing, Vienna, Austria, 2021. URL: <https://www.R-project.org/>.
- J.W. Vaupel, K.G. Manton, and E. Stallard. The impact of heterogeneity in individual frailty on the dynamics of mortality. *Demography*, 16:439–454, 1979. doi: 10.2307/2061224.
- J.W. Vaupel and T.I. Missov. Unobserved population heterogeneity: A review of formal relationships. *Demographic Research*, 31(22):659–686, 2014. doi: 10.4054/DemRes.2014.31.22.
- T.I. Missov and L. Németh. Sensitivity of model-based human mortality measures to exclusion of the Makeham or the frailty parameter. *Genus*, 71(2-3):113–135, 2015.
- F. Ribeiro and T.I. Missov. Revisiting mortality deceleration patterns in a gamma-Gompertz-Makeham framework. In Robert Schoen, editor, *Dynamic Demographic Analysis*, pages 117–146. Springer, Cham, 2016.
- P.H.C. Eilers and B.D. Marx. Flexible smoothing with B-splines and penalties. *Statistical Science*, 112:89–121, 1996. doi: 10.1214/ss/1038425655.
- S. Rizzi, J. Gampe, and P.H.C. Eilers. Efficient estimation of smooth distributions from coarsely grouped data. *American Journal of Epidemiology*, 182(2):138–147, 2015. doi: 10.1093/aje/kwv020.
- C.G. Camarda. MortalitySmooth: An R package for smoothing Poisson counts with P-splines. *Journal of Statistical Software*, 50(1):1–24, 2012. doi: 10.18637/jss.v050.i01.

- M.D. Pascariu, M.J. Dańko, J. Schöley, and S. Rizzi. ungroup: An R package for efficient estimation of smooth distributions from coarsely binned data. *Journal of Open Source Software*, 3(29):937, 2018. doi: 10.21105/joss.00937.
- M.R. Muggeo. Estimating regression models with unknown break-points. *Statistics in Medicine*, 22(19):3055–3071, 2003. doi: 10.1002/sim.1545.
- J.H. Tomal and J.J.H. Ciborowski. Ecological models for estimating breakpoints and prediction intervals. *Ecology and Evolution*, 10(23):13500–13517, 2020. doi: 10.1002/ece3.6955.
- S.C. Patricio, A.J. Sarnaglia, and T.I. Missov. Segmented quantile regression. *Manuscript in preparation*, 2023.
- R. Koenker and J.A.F. Machado. Goodness of fit and related inference processes for quantile regression. *Journal of the American Statistical Association*, 94(448):1296–1310, 1999. doi: 10.1080/01621459.1999.10473882.
- F. Villavicencio and J.M. Aburto. Does the risk of death continue to rise among supercentenarians? In Heiner Maier, Bernard Jeune, and James W. Vaupel, editors, *Exceptional lifespans*, chapter 4, pages 37–48. Springer, Cham, 2021. doi: 10.1007/978-3-030-49970-9_4).
- H. Beltrán-Sánchez, S. Soneji, and E.M. Crimmins. Past, present, and future of healthy life expectancy. *Cold Spring Harbor Perspectives in Medicine*, 5(11):a025957, 2015. doi: 10.1101/cshperspect.a025957.
- F. Villavicencio, M.-P. Bergeron-Boucher, and J.W. Vaupel. Reply to Permanyer et al.: The uncertainty surrounding healthy life expectancy indicators. *Proceedings of the National Academy of Sciences of USA*, 118(46):e2115544118, 2021. doi: 10.1073/pnas.2115544118.

Sex	Country	85	90	95	100	105
Female	Czechia	-0.0195 (34)	-0.0135 (36)	-0.0092 (35)	-0.0070 (36)	-0.0091 (36)
Female	Germany	-0.0137 (20)	-0.0061 (19)	-0.0057 (29)	-0.0046 (29)	0.0047 (29)
Female	Denmark	-0.0108 (49)	-0.0087 (50)	-0.0076 (25)	-0.0011(48)	0.0001 (69)
Female	France	-0.0218 (44)	-0.0162 (43)	-0.0099 (69)	-0.0071 (69)	-0.0077 (69)
Female	U.K.	-0.0139 (41)	-0.0093 (69)	-0.0056 (69)	-0.0004 (34)	0.0021 (37)
Female	Italy	-0.0150 (23)	-0.0056 (15)	-0.0064 (25)	-0.0044 (37)	-0.0025 (69)
Female	Netherlands	-0.0165 (19)	-0.0092 (21)	-0.0052 (22)	-0.0007 (25)	0.0054 (33)
Female	Poland	-0.0228 (24)	-0.0163 (26)	-0.0109 (25)	-0.0014 (61)	0.0006 (61)
Female	Spain	-0.0189 (45)	-0.0127 (49)	-0.0073 (37)	-0.0039 (69)	0.0030 (69)
Female	Sweden	-0.0136 (44)	-0.0080 (49)	-0.0038 (45)	0.0005 (39)	0.0018 (37)
Male	Czechia	-0.0181 (34)	-0.0130 (39)	-0.0073 (29)	-0.0010 (69)	0.0021 (69)
Male	Germany	-0.0129 (14)	-0.0064 (11)	-0.0062 (29)	-0.0026 (29)	0.0047 (29)
Male	Denmark	-0.0194 (17)	-0.0099 (27)	-0.0028 (49)	-0.0026 (44)	0.0017 (69)
Male	France	-0.0209 (22)	-0.0140 (21)	-0.0067 (69)	-0.0037 (69)	0.0022 (69)
Male	U.K	-0.0120 (9)	-0.0144 (21)	-0.0061 (69)	-0.0033 (69)	-0.0004 (69)
Male	Italy	-0.0158 (39)	-0.0085 (30)	-0.0042 (32)	-0.0035 (69)	-0.0018 (69)
Male	Netherlands	-0.0116 (9)	-0.0069 (10)	-0.0045 (26)	-0.0016 (25)	-0.0017 (69)
Male	Poland	-0.0190 (27)	-0.0147 (27)	-0.0071 (20)	0.0028 (51)	0.0016 (61)
Male	Spain	-0.0197 (16)	-0.0101 (46)	-0.0070 (20)	0.0020 (45)	0.0052 (40)
Male	Sweden	-0.0170 (24)	-0.0106 (18)	-0.0063 (18)	-0.0012 (69)	0.0010 (69)

Table 2: Rates of mortality improvement in the last estimated linear segment (CRMI) by country, sex, and age. Statistically significant mortality improvements are presented in blue, while statistically significant mortality increases are designated in red. The scales of blue and red designate the range of the estimated pseudo- R^2 : the darkest blue (e.g., Czech females at age 85) designates values > 0.9 , the second darkest blue (e.g., German females at age 85) designates values from 0.8 to 0.89, the medium blue scale (e.g., German females at age 90) designates values from 0.7 to 0.79, the second lightest blue (e.g., German males at age 95) designates values from 0.6 to 0.69, and the lightest blue (e.g., German females at age 95) designates values from < 0.6 . Darker red (Dutch females at age 105 only) designates pseudo- R^2 from 0.6 to 0.69, while lighter red designates values < 0.6 . The average length (in years) of the last linear segment resulting from fitting a segmented quantile regression to the estimated (by the best-fitting model in Section 3) $\ln m_x$, $x = 85, 90, 95, 100, 105$ is presented in brackets.

Sex	Country	85	90	95	100	105
Female	Czechia	0.94446	0.91669	0.86788	0.71137	0.63356
Female	Germany	0.84144	0.73801	0.38764	0.29491	0.06518
Female	Denmark	0.89872	0.89947	0.93484	0.63266	0.00032
Female	France	0.94686	0.92820	0.78929	0.57838	0.28778
Female	U.K.	0.93664	0.83984	0.72746	0.78539	0.58929
Female	Italy	0.97727	0.97716	0.94163	0.85876	0.09755
Female	Netherlands	0.96395	0.93636	0.90484	0.82543	0.68588
Female	Poland	0.94298	0.92692	0.89830	0.02367	0.01064
Female	Spain	0.95301	0.91274	0.81653	0.26523	0.06264
Female	Sweden	0.94418	0.93067	0.85591	0.73487	0.74821
Male	Czechia	0.90544	0.87914	0.85727	0.01085	0.00387
Male	Germany	0.88607	0.93831	0.60820	0.12348	0.01872
Male	Denmark	0.95580	0.91461	0.72250	0.53745	0.00913
Male	France	0.97862	0.96984	0.74455	0.26614	0.00672
Male	U.K.	0.99089	0.95978	0.73379	0.28027	0.00046
Male	Italy	0.95339	0.95062	0.91282	0.28869	0.00436
Male	Netherlands	0.97923	0.97503	0.88639	0.84766	0.03200
Male	Poland	0.91317	0.91323	0.84501	0.29961	0.00329
Male	Spain	0.97621	0.87631	0.88286	0.58427	0.89671
Male	Sweden	0.96361	0.96310	0.92486	0.05610	0.01627

Table 3: Values of pseudo- R^2 , by age, sex and country, for the last linear year-segment resulting from fitting segmented quantile regression to smoothed logarithmic age-specific death rates.

Appendix: Estimated $\ln m_x$ and segmented quantile regression fits

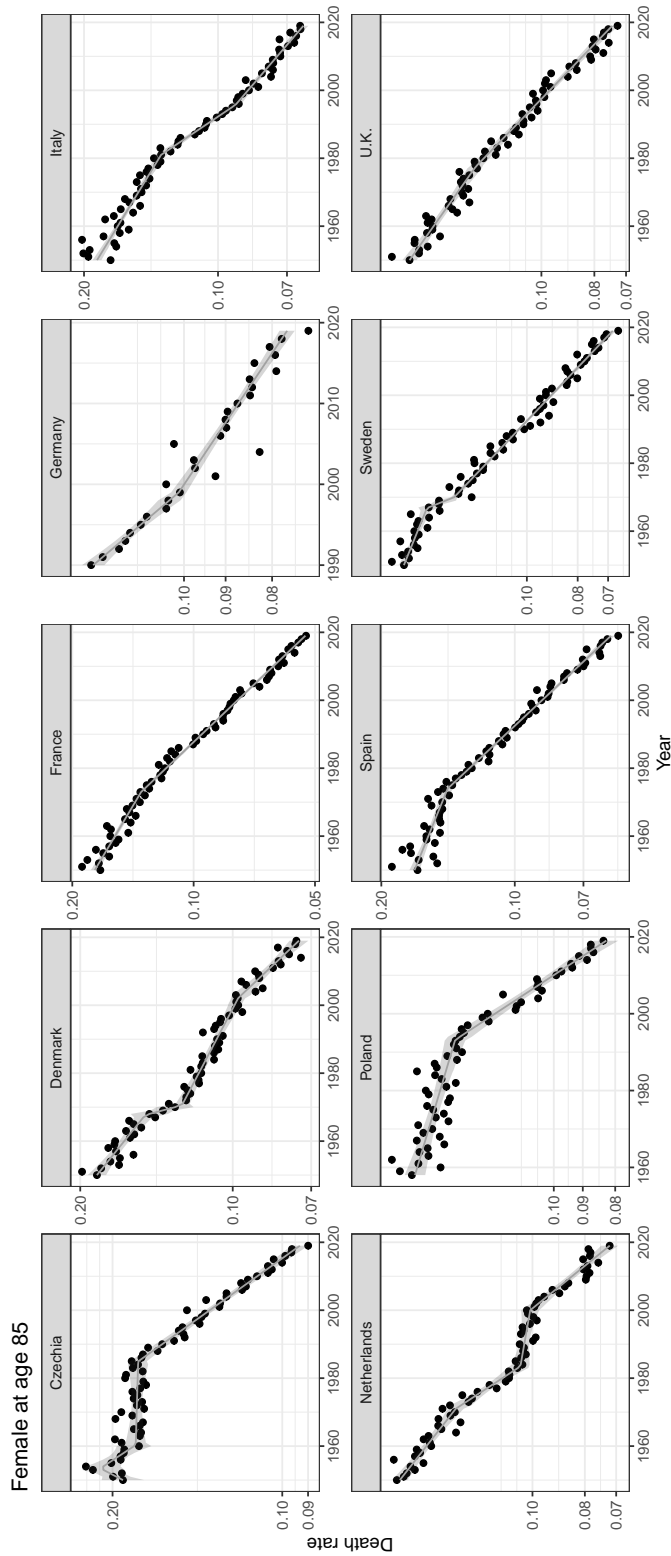


Figure 3: The 1950–2019 time series of female death rates at age 85 (points), obtained by smoothing the death counts at ages 85 and above by the best-fitting procedure (see Table 1) described in Section 3. The solid line represents the best-fitting linear or piecewise linear approximation with its corresponding uncertainty bounds. The existence and number of breakpoints were determined by fitting a segmented quantile regression and testing it (via a likelihood-ratio test) against a linear regression.

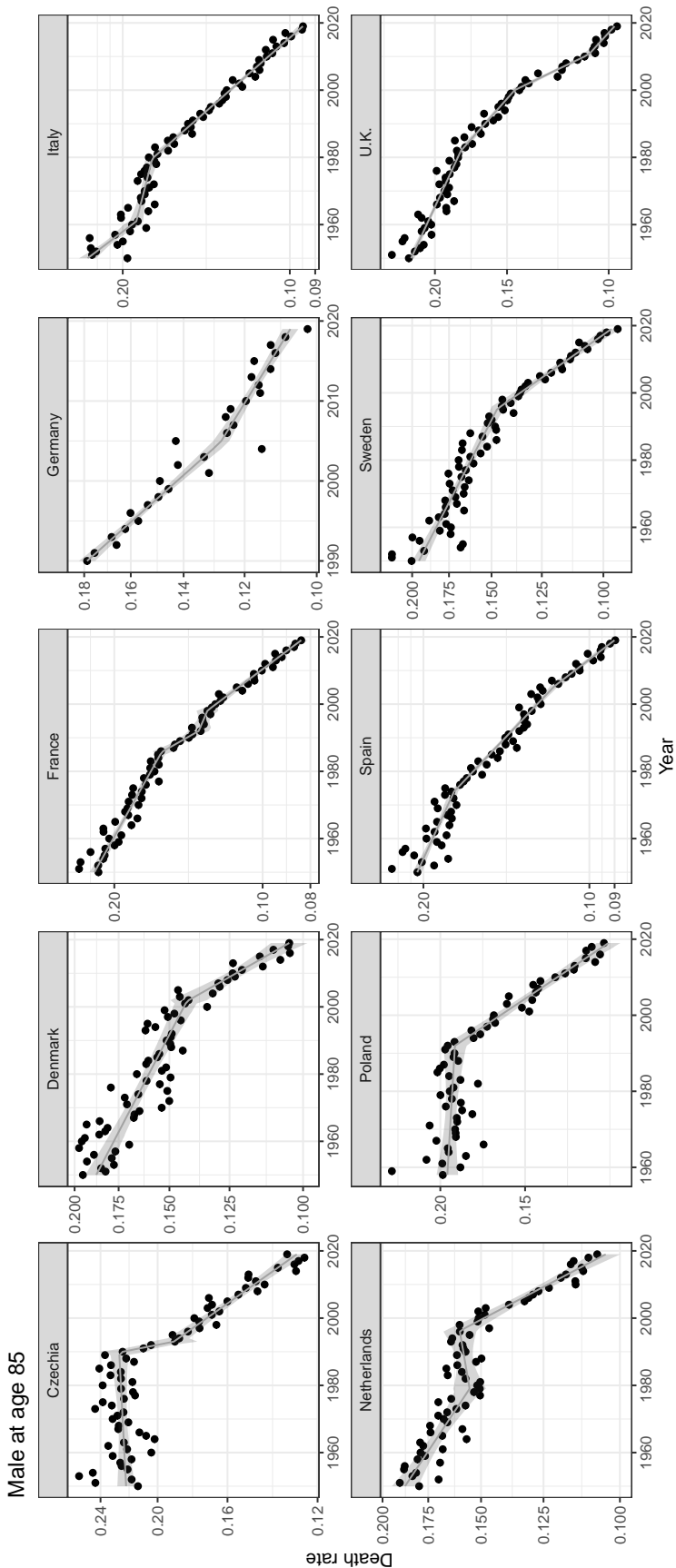


Figure 4: The 1950–2019 (for Germany, 1990–2019) time series of male death rates at age 85 (points), obtained by smoothing the death counts at ages 85 and above by the best-fitting procedure (see Table 1) described in Section 3. The solid line represents the best-fitting linear or piecewise linear approximation with its corresponding uncertainty bounds. The existence and number of breakpoints were determined by fitting a segmented quantile regression and testing it (via a likelihood-ratio test) against a linear regression.

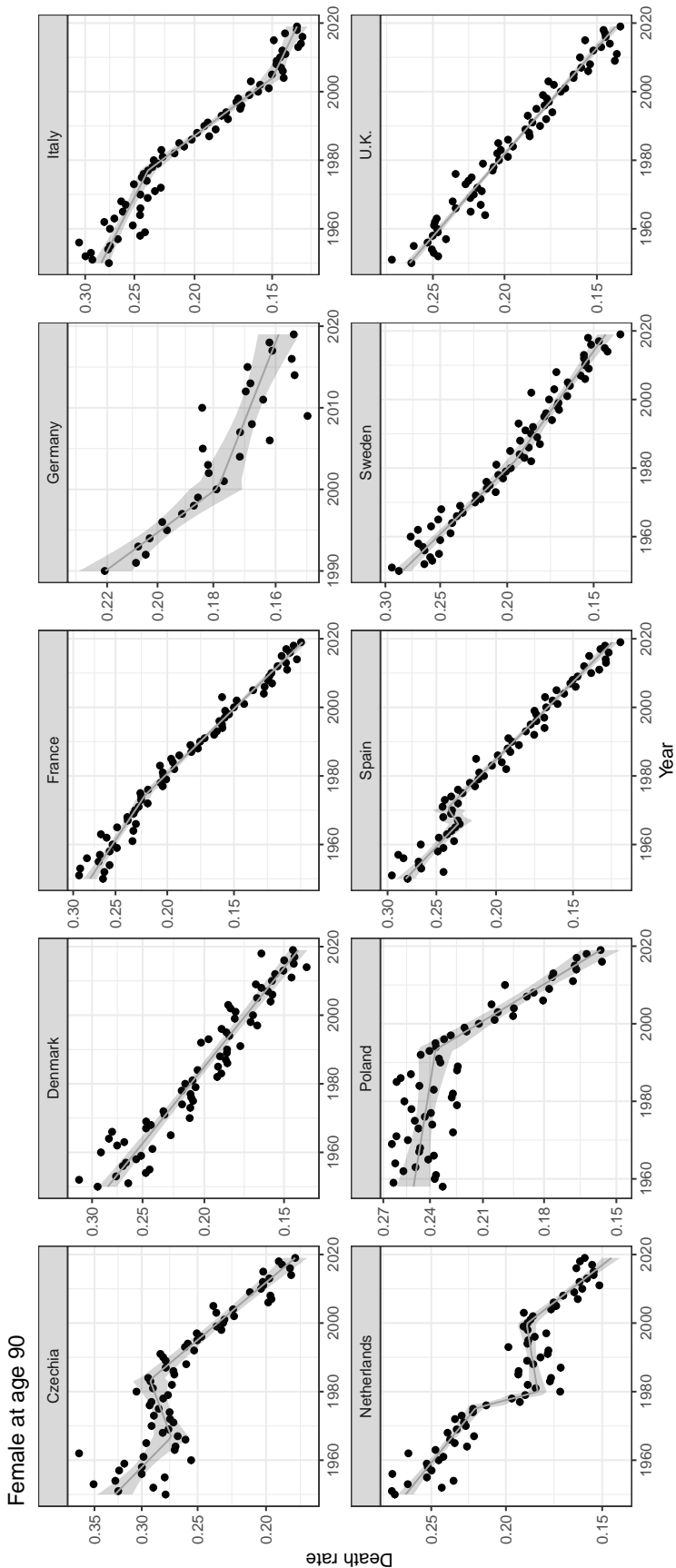


Figure 5: The 1950–2019 (for Germany, 1990–2019) time series of female death rates at age 90 (points), obtained by smoothing the death counts at ages 85 and above by the best-fitting procedure (see Table 1) described in Section 3. The solid line represents the best-fitting linear or piecewise linear approximation with its corresponding uncertainty bounds. The existence and number of breakpoints were determined by fitting a segmented quantile regression and testing it (via a likelihood-ratio test) against a linear regression.

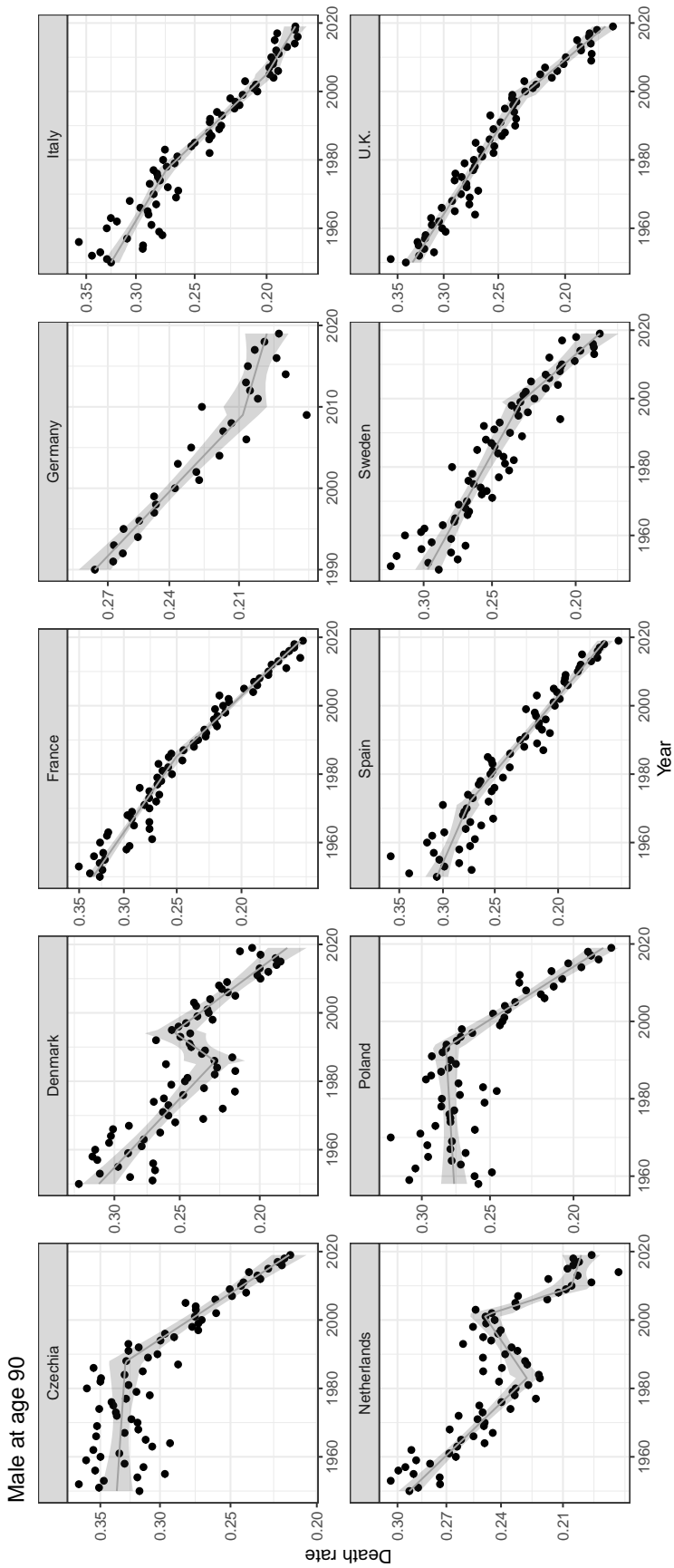


Figure 6: The 1950–2019 (for Germany, 1990–2019) time series of male death rates at age 90 (points), obtained by smoothing the death counts at ages 85 and above by the best-fitting procedure (see Table 1) described in Section 3. The solid line represents the best-fitting linear or piecewise linear approximation with its corresponding uncertainty bounds. The existence and number of breakpoints were determined by fitting a segmented quantile regression and testing it (via a likelihood-ratio test) against a linear regression.

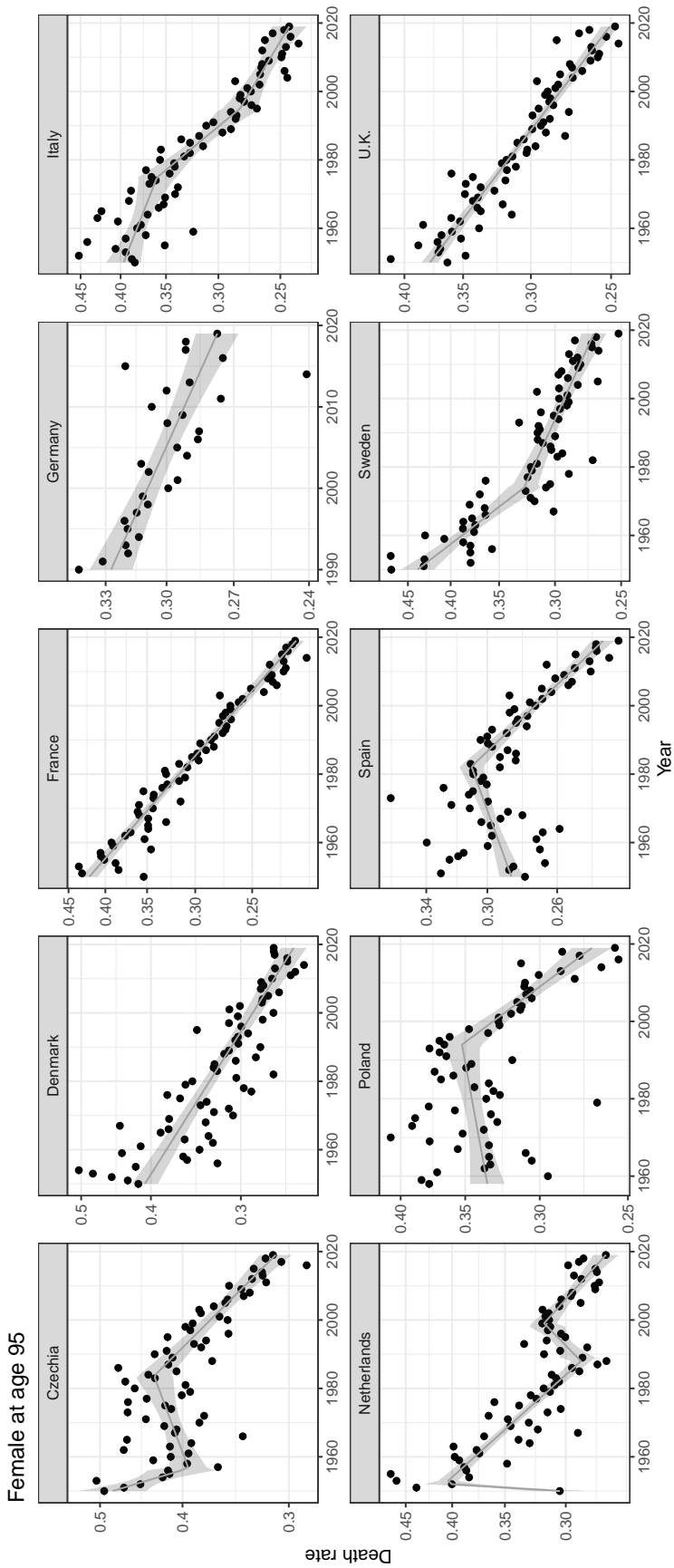


Figure 7: The 1950–2019 (for Germany, 1990–2019) time series of female death rates at age 95 (points), obtained by smoothing the death counts at ages 85 and above by the best-fitting procedure (see Table 1) described in Section 3. The solid line represents the best-fitting linear or piecewise linear approximation with its corresponding uncertainty bounds. The existence and number of breakpoints were determined by fitting a segmented quantile regression and testing it (via a likelihood-ratio test) against a linear regression.

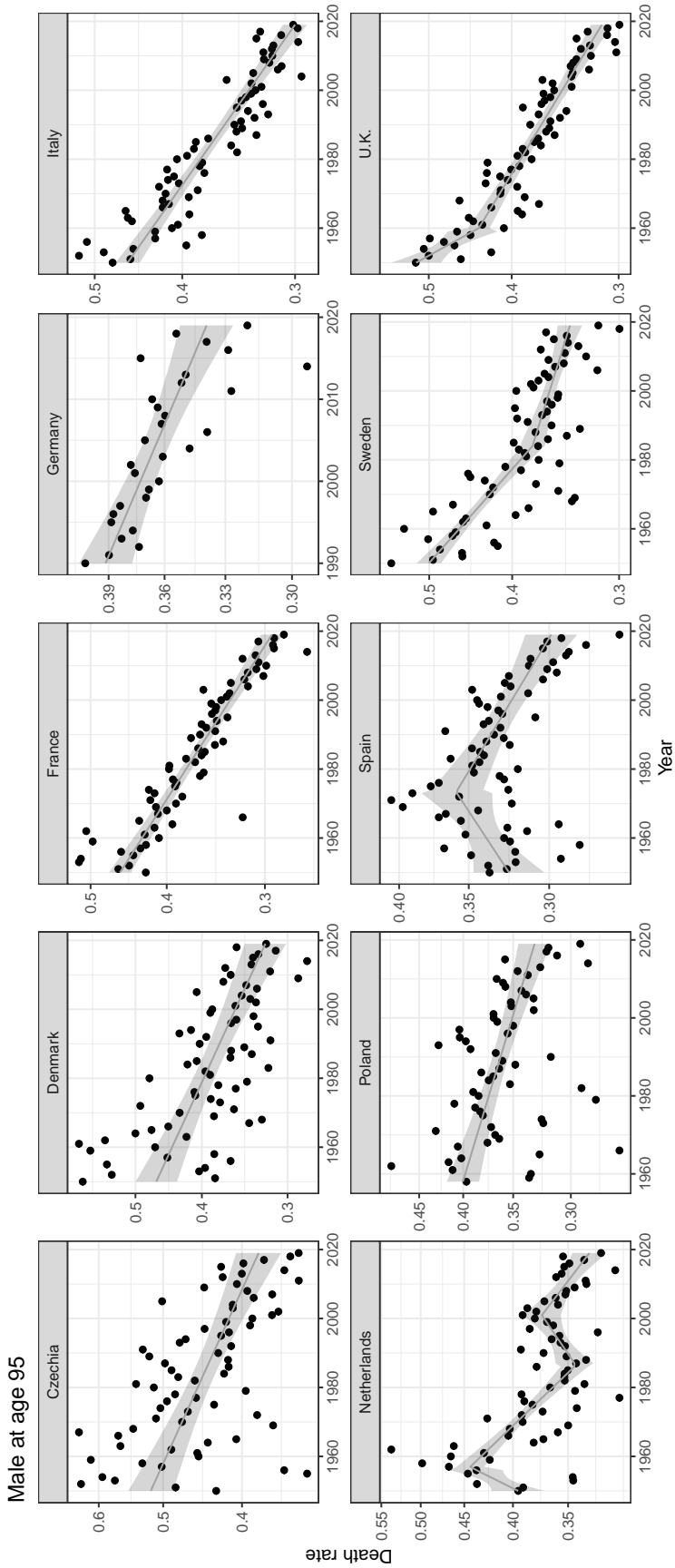


Figure 8: The 1950–2019 (for Germany, 1990–2019) time series of male death rates at age 95 (points), obtained by smoothing the death counts at ages 85 and above by the best-fitting procedure (see Table 1) described in Section 3. The solid line represents the best-fitting linear or piecewise linear approximation with its corresponding uncertainty bounds. The existence and number of breakpoints were determined by fitting a segmented quantile regression and testing it (via a likelihood-ratio test) against a linear regression.

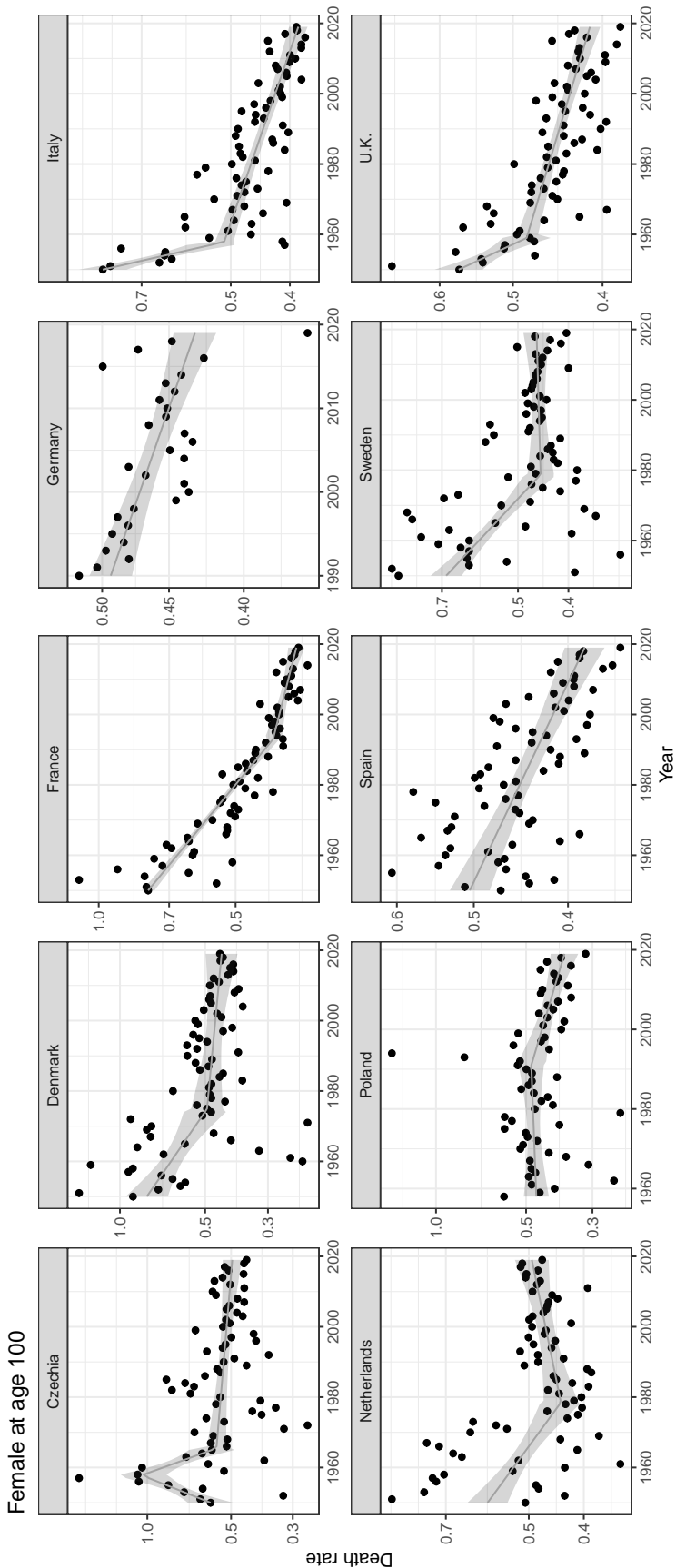


Figure 9: The 1950–2019 (for Germany, 1990–2019) time series of female death rates at age 100 (points), obtained by smoothing the death counts at ages 85 and above by the best-fitting procedure (see Table 1) described in Section 3. The solid line represents the best-fitting linear or piecewise linear approximation with its corresponding uncertainty bounds. The existence and number of breakpoints were determined by fitting a segmented quantile regression and testing it (via a likelihood-ratio test) against a linear regression.

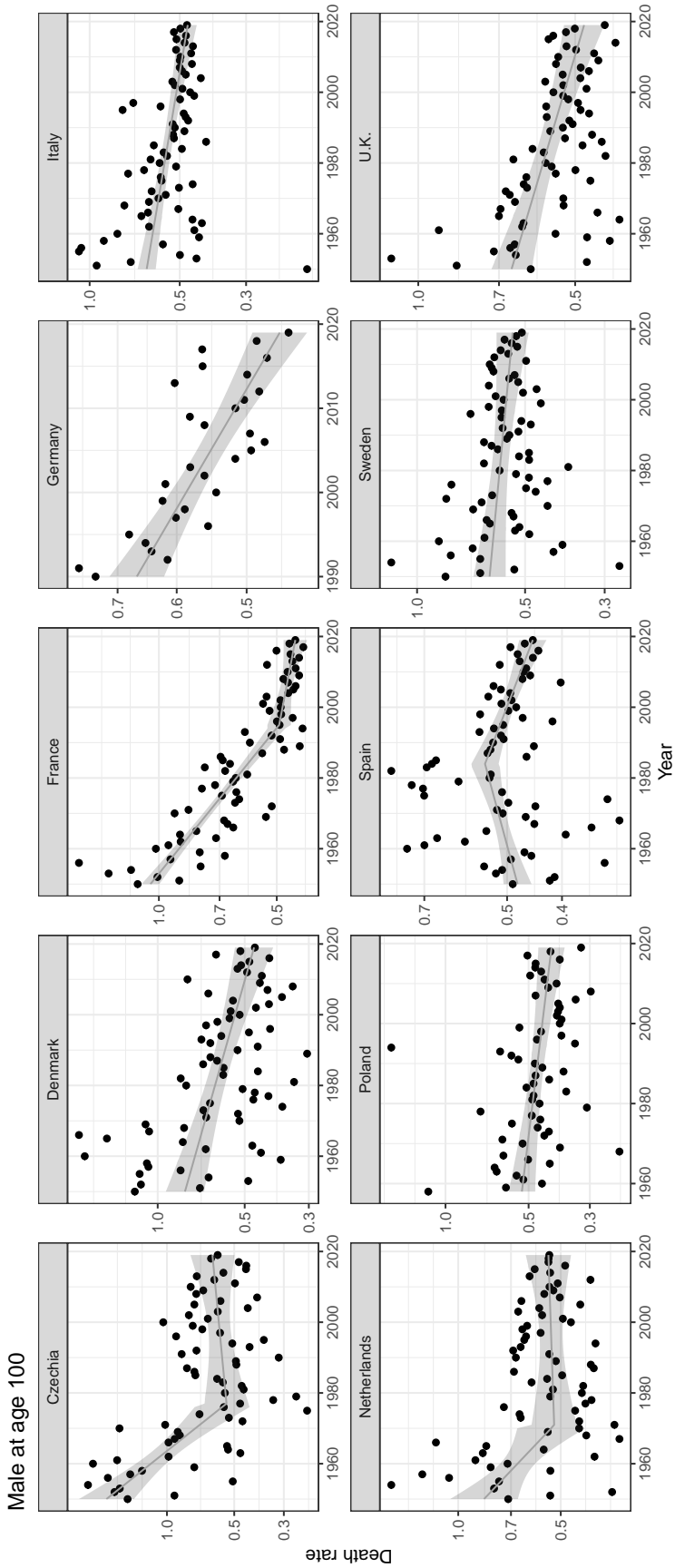


Figure 10: The 1950–2019 (for Germany, 1990–2019) time series of male death rates at age 100 (points), obtained by smoothing the death counts at ages 85 and above by the best-fitting procedure (see Table 1) described in Section 3. The solid line represents the best-fitting linear or piecewise linear approximation with its corresponding uncertainty bounds. The existence and number of breakpoints were determined by fitting a segmented quantile regression and testing it (via a likelihood-ratio test) against a linear regression.

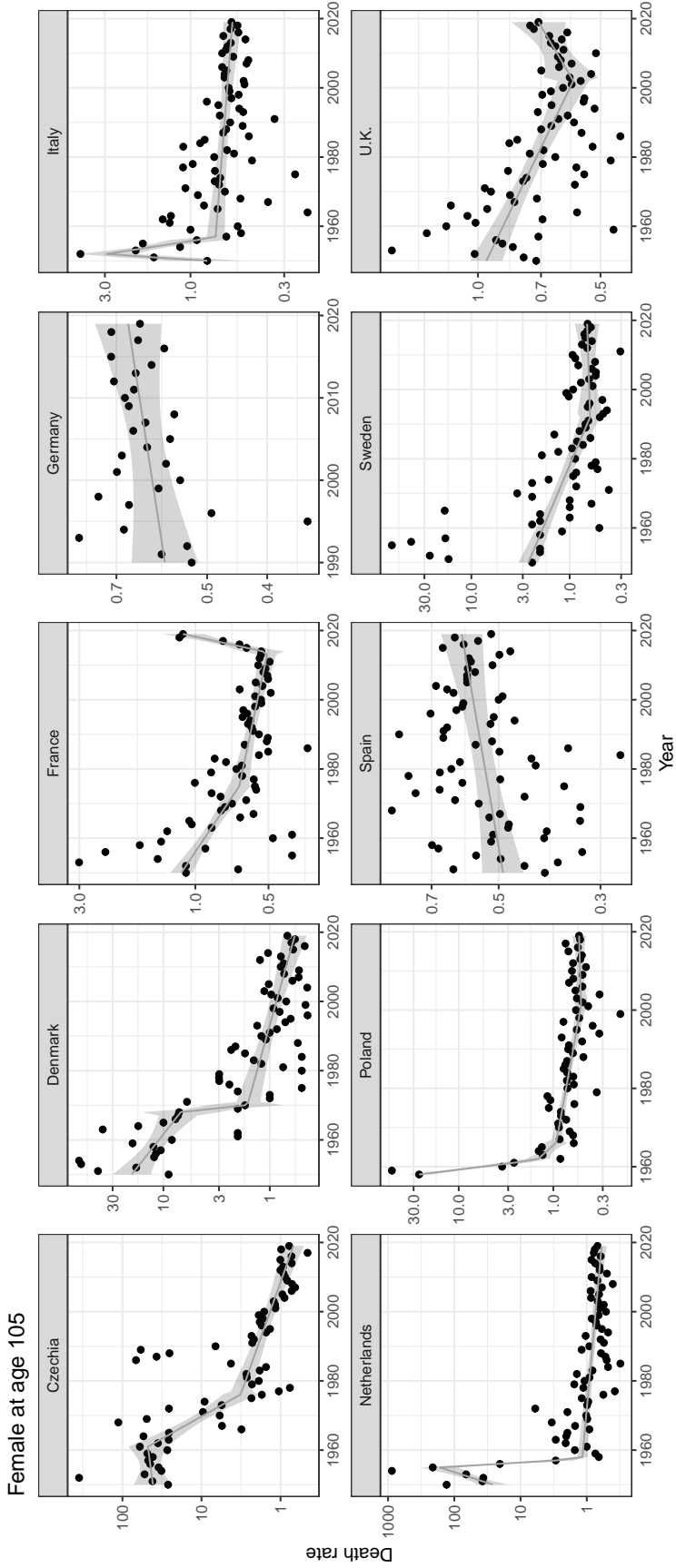


Figure 11: The 1950–2019 (for Germany, 1990–2019) time series of female death rates at age 105 (points), obtained by smoothing the death counts at ages 85 and above by the best-fitting procedure (see Table 1) described in Section 3. The solid line represents the best-fitting linear or piecewise linear approximation with its corresponding uncertainty bounds. The existence and number of breakpoints were determined by fitting a segmented quantile regression and testing it (via a likelihood-ratio test) against a linear regression.

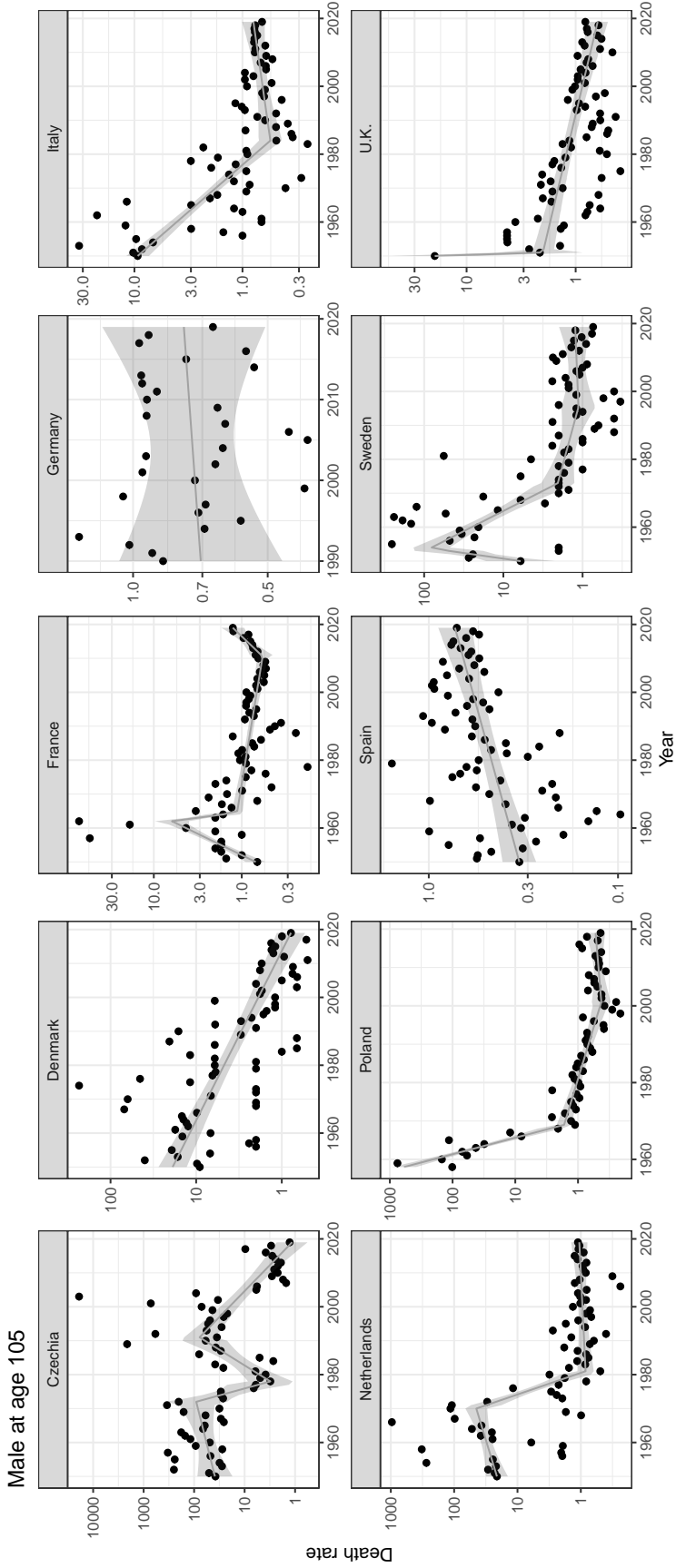


Figure 12: The 1950–2019 (for Germany, 1990–2019) time series of male death rates at age 105 (points), obtained by smoothing the death counts at ages 85 and above by the best-fitting procedure (see Table 1) described in Section 3. The solid line represents the best-fitting linear or piecewise linear approximation with its corresponding uncertainty bounds. The existence and number of breakpoints were determined by fitting a segmented quantile regression and testing it (via a likelihood-ratio test) against a linear regression.